

Label and Sample: Efficient Training of Vehicle Object Detector from Sparsely Labeled Data

Xinlei Pan
UC Berkeley
Berkeley, CA, USA 94720
xinleipan@berkeley.edu

Sung-Li Chiang
UC Berkeley
Berkeley, CA, USA 94720
slchiang@berkeley.edu

John Canny
UC Berkeley
Berkeley, CA, USA 94720
canny@berkeley.edu

Abstract

Self-driving vehicle vision systems must deal with an extremely broad and challenging set of scenes. They can potentially exploit an enormous amount of training data collected from vehicles in the field, but the volumes are too large to train offline naively. Not all training instances are equally valuable though, and importance sampling can be used to prioritize which training images to collect. This approach assumes that objects in images are labeled with high accuracy. To generate accurate labels in the field, we exploit the spatio-temporal coherence of vehicle video. We use a near-to-far labeling strategy by first labeling large, close objects in the video, and tracking them back in time to induce labels on small distant presentations of those objects. In this paper we demonstrate the feasibility of this approach in several steps. First, we note that an optimal subset (relative to all the objects encountered and labeled) of labeled objects in images can be obtained by importance sampling using gradients of the recognition network. Next we show that these gradients can be approximated with very low error using the loss function, which is already available when the CNN is running inference. Then, we generalize these results to objects in a larger scene using an object detection system. Finally, we describe a self-labeling scheme using object tracking. Objects are tracked back in time (near-to-far) and labels of near objects are used to check accuracy of those objects in the far field. We then evaluate the accuracy of models trained on importance sampled data vs models trained on complete data.

1. Introduction

Autonomous driving is receiving enormous development effort with many companies predicting large-scale commercial deployment in 2-3 years [35]. One of the most important features of autonomous driving vehicles is the ability to interpret the surroundings and perform complex

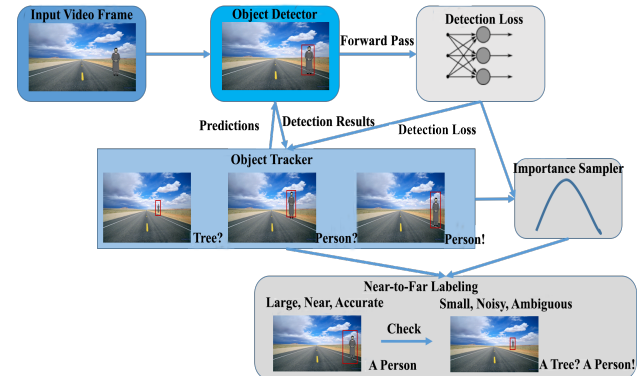


Figure 1. Overview of our method. Given a sequence of video frame inputs, the object detection network first detects objects in a frame, the forward pass step. Then the loss of the images are calculated. Both detection results and loss will be sent to object tracker which keeps a list of active objects. The importance sampler determines whether to save the detection or not based on the loss. Furthermore, the near-to-far labeling step checks the accuracy of objects that are in the far field using the classification result of near field objects, where we believe near field objects are larger and the classification is more accurate.

perception task such as the detection and recognition of lanes, roads, pedestrians, vehicles, and traffic signs [27]. Recently, the growth of Convolutional Neural Networks (CNNs), and large labeled data sets [8, 11] have led to tremendous progress in object detection and recognition [14, 15, 26, 20]. It is now possible to detect objects with high accuracy [26, 25, 20].

Videos collected in-vehicle have a great potential to improve model quality (through offline training) but at the scales achievable in a few years (billions to trillions of hours of video), training on all the data is completely impractical. Nor is it desirable - most images contain “typical” content and objects that are recognized with good accuracy. These models contribute little to the final model. But it is the less common “interesting” images that are most important for training (i.e. images containing objects that are

mis-classified, or classified with low confidence). To benefit from these images, it's still important to have accurate label information. The images of distance objects in isolation are not good for this purpose - by definition they contain objects which are difficult to label automatically. But we can use particular characteristics of vehicle video: namely that most of the time (vehicle moving forward), objects gradually grow and become clearer and easier to recognize. We exploit this coherence by tracking objects back in time and using near, high-reliability labels to label more distant objects. We demonstrate this process on a hand-labeled dataset [13] which only has a small fraction of total frames labeled and also has short length video clips that can be used for object tracking. We show that we can extend the labelled data using near-to-far tracking strategy, and importance sampling can be used to refine the automatically labeled dataset to improve its quality.

To automate far-object tracking, we need both single-image object detection and between-image tracking. While these two modules can be used separately, we designed a strategy to nicely combine them together. Specifically we used a Faster-RCNN object detector [26] and Kalman filtering to track objects. We use predicted object positions from tracking to augment the Faster-RCNN's region proposals, and then use the Faster-RCNN's bounding box regression to correct the object position estimates. The result is that we can track and persist object layers much further into the distance where it might be hard for Faster-RCNN to give accurate object region proposal.

The automatically-generated labels are then used to compute the importance of each image. As shown in [2], an optimal model is obtained when images are importance sampled using the norm of the back-propagated gradient magnitude for the image. While computing the full back-propagated gradients in vehicle video systems would be very expensive, we can actually use the loss function as a surrogate for gradient as it is easier to obtain. We further show in our experiments that the loss function can be a approximate of the gradient norm. Importance sampling for training data filtering is also described in [7].

Contributions. Starting with a sparsely labeled video dataset, we combine object tracking and object detection to generate new labeled data, and then use importance sampling for data reduction. The contributions of this paper are: 1) We show that near-to-far object tracking can produce useful training data augmentation. 2) Empirically, gradient norm can be approximated by loss function and last layer gradient norm in deep neural networks. 3) Importance sampling produces large reductions in training data and training time and modest loss of accuracy.

2. Related Work

Semi-Supervised Data Labeling. With the large amount of sparsely labeled image datasets, some work has been done in the field of semi-supervised object detection and data labeling [34, 31, 18, 6]. These work try to learn a set of similar attributes for image classes [31, 6] to label new datasets, or to cluster similar images [18], or perform transfer learning to recognize similar types of objects [34]. However, these work are typically suitable for image dataset where they process images individually and do not consider the temporal continuity of video dataset for semi-supervised learning. Semi-supervised learning for video dataset is also described in [19, 24, 33]. While their performance is good, they assume labeling the salient object in a video and thus do not apply well to multi-object detection or tracking case. A large body of work has also been done in the field of tracking-by-detection [3, 23, 16, 17, 5]. However, they either assume the possibility of negative data being sampled from around the object or they do not use the special characteristic of driving video that objects in the near field are easier to be detected than objects in the far field. In addition, these naive combinations of tracking and detection may introduce additional noise in labeling images. Also, tracking tends to drift away in the long run and the related data association is also very challenging [3]. In the work of [21], they proposed to use semi-supervised learning to label large video datasets by tracking multiple objects in videos. However, their application scenario is not driving video dataset and the object they detect only include cars. In addition, their focus is on short term tracking of objects and they do not require short tracklets to be associated with each other. Therefore, the applicability of their method is limited especially when there are multiple categories of objects in a scene, since ignoring the data association part would be problematic if the goal is to label multiple categories of objects. In our work, we do consider the problem of data association and we use object tracker's prediction as the region proposal for object detector to provide more accurate bounding box annotation. However, similar to the work of [21], we do not perform long-run tracking to prevent the tracker from drifting away. We also use near-to-far labeling to help correct the detector's classification results.

Importance Sampling. Importance sampling is a well-known technique used for reducing the variance when estimating properties of a particular distribution while only having samples generated from another distribution [22, 28]. The work of [38] studied the problem of improving traditional stochastic optimization with importance sampling, where they improved the convergence rate of prox-SMD [9, 10] and prox-SDCA [29] by reducing the stochastic variance using importance sampling. The work of [2] improves over [38] by incorporating stochastic gradient descent and deep neural networks. Also there are some work in using

importance sampling for minibatch SGD [7], where they proposed to use importance sampling to do data sampling in minibatch SGD and this can improve the convergence rate of SGD. The idea of hard negative example mining is also highly related to our work. As shown in [30] where they presented an approach to perform efficient object detection training by training on an optimally sampled bounding boxes according to their gradient.

As for self-driving vehicles' vision system training, we typically do not know the ground truth distribution of the data, which are the images or video data captured by cameras. Thus, importance sampling will be very useful in estimating the properties of the data from a data-driven sampling scheme. The work of [36] and [12] proposed to use importance sampling for visual tracking, but their focus was not on reducing the training data amount and creating labeled data using visual tracking. In our work, we use importance sampling to obtain an optimal set of data so that our training efficiency is high as we train on the most informative data. The information that each image carries is characterized by their detection loss, which is reasonably suitable in our case as images with high loss are usually images that are difficult for the current detector.

3. Methods

Our approach for creating labeled data and performing data reduction by importance sampling can be divided into two parts. First of all, based on the sparsely labeled image frames, we initialize object tracker by incorporating Kalman-filter algorithm [37] and use the tracker to predict bounding box of objects in the previous (since we predict back in time) frame. We then use the prediction as region proposal input and send this to object detection module. Based on the region proposal received, the object detection module trained on sparsely labeled data will do a bounding box regression to get the final bounding box and detection loss. The object tracker further matches new detections to existing trackers or create new trackers if the new detection cannot match any of the existing trackers. The near-to-far labeling module will double check object detection results within each tracker to use the classification results of objects in the near field which are more accurate to check the results of objects in the far field. The bounding box produced by the object detection module are used as labels for those unlabeled video frames. The detection loss will be used as the sampling weights for importance sampling. Secondly, based on the detection loss recorded in the first part, the importance sampler will sample an optimal subset of labeled images and these selected labeled images will be used as the training data to train a new object detector.

The system architecture is shown in figure 1. Here, we first describe the framework of semi-supervised data labeling followed by the data reduction using the importance

sampling framework.

3.1. Semi-supervised Data Labeling

Object Tracking. Starting with a few sparsely annotated video frames, we first trained an object detection network using Faster-RCNN [26]. By using Kalman filter [37], we initialize object trackers with the ground truth labeled frames. The specific object tracking framework we use is similar to that of [1], where the state of the tracker includes 7 parameters, namely, the center position of the bounding box x, y , the scale s (the area of the bounding box) and aspect ratio r of the bounding box (the ratio of the width over the height of the bounding box), and the rate of change of the center position v_x, v_y and scale v_s of the bounding box. We follow the assumption in [1] that the aspect ratio of the bounding box does not change over time. The measurement is just the first four parameters of the state vector.

$$\text{state} = [x, y, s, r, v_x, v_y, v_s]$$

$$\text{measurement} = [x, y, s, r]$$

We always use ground truth labeled bounding box to initialize object trackers, and the tracking is done from the near field to the far field, which means the video is played in the opposite direction as it was collected, so that at the very beginning, the camera is close to the labeled objects and at the very end the camera is far away from the the object. Therefore, it is reasonable to believe that the classification and detection results for objects in the near field are more reliable while there is more noise in the detection results for object in the far field.

Prediction as Region Proposal. After the trackers are initialized with ground truth bounding box, based on the principle of a Kalman filter, predictions of bounding boxes of the objects being tracked will be calculated. These predictions will be used as a hint for the object detection network to produce new bounding boxes in the next frame. The network we used for object detection is Faster-RCNN [26], which is composed of a region proposal network (RPN) and object detection network Fast-RCNN [15]. Usually the RPN will be used as the region proposer, however, as we already have the prior information of where the object might be, we can directly use this information to help the object detection network avoid uncertainty in region proposal. This part corresponds to the `get_new_detection` method in algorithm 1.

Matching Tracker with Detections. Given the predictions sent by the object tracker, the object detection network will produces a set of candidate bounding boxes in the next frame and the object tracker will try to match the existing trackers and the new detections using linear assignment. We also use intersection over Union (IoU) to filter out detection-tracker pairs that do not have IoU values higher

Description: Update object bounding box label for a single track-back-in-time step.

Input: \mathcal{T} : the list of active trackers; l_ϵ : threshold of detection loss, save a detection if the detection loss is larger than this threshold; \mathcal{K} : Kalman filter; \mathcal{D} : object detector; n : limit of steps to retain a tracker;

Result: \mathcal{R} (collections of detections to be saved, a detection is a bounding box containing state information $(x, y, s, r, label)$ where $label$ is the class of the object)

Initialize: $\mathcal{R} = \emptyset, \mathcal{R}' = \emptyset, \mathcal{P}_m = \emptyset, \mathcal{P}_m$ is the matched pairs of detection and tracker.

```

for  $\forall T \in \mathcal{T}$  do
  /* Tracking back in time */
   $s = \text{predict\_state}(T, \mathcal{K});$ 
  /* Use  $s$  (prediction of RoI) as region proposal */
   $d = \text{get\_new\_detection}(s, \mathcal{D});$  % Refer to section 3.1
   $\mathcal{R}' = \mathcal{R}' \cup d;$ 
end
for  $\forall d, T \in \mathcal{R}', \mathcal{T}$  do
  Match  $d, T$ 
  if  $d, T$  can match then
     $\mathcal{P}_m = \mathcal{P}_m \cup (d, T);$ 
  end
end
 $\mathcal{R}'_{um} = \{d; d \in \mathcal{R}' \ \& \ d \notin \mathcal{P}_m\}$  (get unmatched  $d$ );
 $\mathcal{T}_{um} = \{T; T \in \mathcal{T} \ \& \ T \notin \mathcal{P}_m\}$  (get unmatched  $T$ );
for  $\forall (d, T) \in \mathcal{P}_m$  do
  Update tracker  $T$  using  $d$  using Kalman Filter;
  Using historical records in trk to check the accuracy of this new detection  $d$ ;
   $\mathcal{R} = \mathcal{R} \cup d;$ 
end
for  $\forall$  unmatched  $d \in \mathcal{R}'_{um}$  do
   $T = \text{init\_new\_tracker}(d);$ 
   $\mathcal{R} = \mathcal{R} \cup d;$ 
end
for  $\forall$  unmatched  $T \in \mathcal{T}_{um}$  do
  if  $T$  has not been updated for more than  $n$  times then
    Remove  $T$  from  $\mathcal{T}$ 
  end
end
for  $\forall d \in \mathcal{R}$  do
  if  $d$  has loss  $> l_\epsilon$  then
    mark this  $d$  to be saved
  end
end
return  $\mathcal{R}$ 

```

Algorithm 1: Object Tracking and Labeling Algorithm

Description: Match detections with trackers.

Input: \mathcal{R}' : object detection bounding boxes, $d = [x_1, y_1, x_2, y_2]$; \mathcal{T} : trackers;

Result: Matched detection and tracker pairs \mathcal{P}_m ; Unmatched detections \mathcal{R}'_{um} ; Unmatched Trackers \mathcal{T}_{um} ;

```

if  $\text{len}(\mathcal{T}) == 0$  then
   $\mathcal{P}_m = \emptyset; \mathcal{R}'_{um} = \mathcal{R}'; \mathcal{T}_{um} = \emptyset;$ 
  return  $\mathcal{P}_m, \mathcal{R}'_{um}, \mathcal{T}_{um}.$ 
end
 $M = \text{An all-zeros matrix of size } [\text{len}(\mathcal{R}'), \text{len}(\mathcal{T})].$ 
for  $i$  from 1 to  $\text{len}(\mathcal{R}')$  do
  for  $j$  from 1 to  $\text{len}(\mathcal{T})$  do
     $M[i, j] = \text{IntersectionOverUnion}(\mathcal{R}'[i], \mathcal{T}[j])$ 
  end
end
 $M2 = \text{linear\_assignment}(M[i, j]);$ 
for  $i$  from 1 to  $\text{len}(\mathcal{R}')$  do
  if  $i \notin M2[:, 0]$  then
     $\mathcal{R}'_{um} = \mathcal{R}'_{um} \cup \mathcal{R}'[i]$ 
  end
end
for  $j$  from 1 to  $\text{len}(\mathcal{T})$  do
  if  $j \notin M2[:, 1]$  then
     $\mathcal{T}_{um} = \mathcal{T}_{um} \cup \mathcal{T}[j]$ 
  end
end
for  $i, j \in M2$  do
   $\mathcal{P}_m = \mathcal{P}_m \cup (\mathcal{R}'[i], \mathcal{T}[j]).$ 
end
return  $\mathcal{P}_m, \mathcal{R}'_{um}, \mathcal{T}_{um}.$ 

```

Algorithm 2: Match Detections with Trackers

than a pre-defined threshold. After finishing detection-tracker matching, the state of valid trackers will be updated, and trackers that remain inactive (not being updated) for a certain steps will be removed from the trackers list. Now we finished one step of object tracking and labeling. The bounding boxes produced by object detection network will be used as labels for those unlabeled video frames. The more detailed algorithm description for one step of tracking and labeling is shown in algorithm 1. Matching trackers with detections is further described in algorithm 2.

The *tracker* is a class containing state of the current object being tracked and methods for updating object's state given ground truth state of the object. A detailed implementation of the tracker class can be found in [4].

Near-to-Far Labeling. Another key ingredient of our approach is the near-to-far labeling scheme. Consider the case that we are tracking an object from far to near field. When the image is far away from our current location, the object could be very small or blurred in the image, which

makes it very difficult to be correctly classified. As the object approaches the vehicle, the detection network has a higher confidence to correctly classify this object. As we trust object detection results in the near field, if object detection results of the same object being tracked in the far field differ from that in the near field, we can use the detection results in the near field to correct that. To do this, we restrict object tracker’s initialization only to ground truth bounding boxes so as to avoid the additional noise introduced by imperfect object detection network. In case the classification of objects in the far field diverges, we use the detection result of the same tracker in the near field to correct that. Examples of near-to-far labeling are shown in figure 4.

3.2. Sampling an Optimal Subset of Images

Inspired by the idea of importance sampling [2], we can select an optimal subset of the data by sampling the data according to importance sampling probability distribution so that the variance of the sampled data is minimized under an expected size of sampled data. Here, the sampling distribution is proportional to the object detection loss of each image. Images with higher loss obtain more importance as they provide more useful information for accurate object detection.

In our case, we are interested in estimating the expectation of $f(x)$ based on a distribution $p(x)$, where $f(x)$ is the detection loss of each image, $p(x)$ denotes the image distribution and x denotes a particular image with an object detection loss. The problem is expressed by the following equation,

$$\int p(x)f(x)dx = \mathbb{E}_{p(x)}[f(x)] \approx \frac{1}{N} \sum_{n=1}^N f(x_n), \quad (1)$$

where $x_n \sim p(x)$. However, usually we do not know the ground truth distribution of the data $p(x)$, so we rely on a sampling proposal $q(x)$ to unbiasedly estimate this expectation, with the requirement that $q(x) > 0$ whenever $p(x) > 0$. This is commonly known as importance sampling:

$$\int p(x)f(x)dx = \mathbb{E}_{p(x)}[f(x)] = \mathbb{E}_{q(x)}\left[\frac{p(x)}{q(x)}f(x)\right]. \quad (2)$$

It has been proved in [2] that the variance of this estimation can be minimized when we have,

$$q^*(x) \propto p(x)|f(x)|. \quad (3)$$

Defining $\tilde{q}^*(x_i)$ as the unnormalized optimal probability weight of image x_i , it is obvious that images with a larger detection loss should have a larger weight. Although we do not know $p(x)$, we have access to a dataset $\mathcal{D} = \{x_n\}_{n=1}^N$ sampled from $p(x)$. Therefore, we can obtain $q^*(x)$ by associating the unnormalized probability weight $\tilde{q}^*(x_n) =$

$|f(x_n)|$ to every $x_n \in \mathcal{D}$, and to sample from $q^*(x)$ we just need to normalize these weights:

$$q^*(x_n) = \frac{\tilde{q}^*(x_n)}{\sum_{i=1}^N \tilde{q}^*(x_i)} = \frac{|f(x_n)|}{\sum_{i=1}^N |f(x_i)|} \quad (4)$$

where $f(x_i)$ is the loss of input x_i . To reduce the total number of data instances used for estimating $\mathbb{E}_{p(x)}[f(x)]$, we draw M samples from the whole N data instances ($M \ll N$) based on a multinomial distribution where $(q^*(x_1), \dots, q^*(x_N))$ are the parameters of this multinomial distribution. Based on the discussion above, we obtained an estimation of $\mathbb{E}_{p(x)}[f(x)]$ which has least variance compared to all cases where we draw M samples from the entire N data set. We further provide some prove in the appendix.

3.3. Measuring Variance Reduction Efficiency

Once we get the sampling distribution $q^*(x_i)$, we then perform the importance sampling. Images with a higher detection loss will get higher likelihood to be sampled. We, further, measure how efficient that we estimate the detection loss distribution. Since the goal of using importance sampling approach here is to reduce the variance while estimating properties of the data from a subset of the data.

To show that the expectation of loss estimated from the sampled images have close variance with loss variance estimated from all images, we computed a relative variance value. This value is the ratio of whole data set detection loss variance over sampled images’ detection loss variance.

Suppose the data set is $\mathcal{D} = \{x_n\}_{n=1}^N$, and we can get detection loss $g(x_i)$ given individual input x_i . In order to calculate the relative variance more easily, we will first normalize $g(x)$. Then, we define the sampling probability of image x_i when we expect to sample M out of N images ($M < N$) as,

$$q(x_i) = \min \left[1, \frac{M|g(x_i)|}{\sum_{i=1}^N |g(x_i)|} \right] \quad (5)$$

taking the minimum compared with 1 is to ensure that the probability of sampling image x_i can not be larger than 1, which happens when $\frac{M|g(x_i)|}{\sum_{i=1}^N |g(x_i)|}$ is saturated. Note that, when the sampling probability is 1, we should sample this image. With the scaled sampling weight $\frac{M|g(x_i)|}{\sum_{i=1}^N |g(x_i)|}$, we change M so that we can get different numbers of images out of the entire image date. Typically, choosing a M such that the sample gradient norm variance is close to whole data gradient norm variance. Since the data are in the discrete space, the relative variance is defined as,

$$R = \frac{\sum_{i=1}^N |g(x_i)|^2}{\sum_{i=1}^N |g(x_i)|^2 / q(x_i)}. \quad (6)$$



Figure 2. Bounding box generated by using strategies mentioned in experiment 1 (left 1 and 2) and experiment 2(right 1 and 2)

	Pedestrian			Car			Cyclist			mAP
	Easy	Medium	Hard	Easy	Medium	Hard	Easy	Medium	Hard	
Ground Truth (GT)	80.6	68.8	61.0	94.1	78.8	69.3	88.1	78.8	73.6	77.0
New Labeled (NL) & GT	69.2	58.4	50.8	83.4	63.2	53.1	68.3	56.6	52.9	61.8
Sampled NL & GT	71.3	62.7	54.1	75.8	61.5	51.6	77.5	66.0	61.3	64.6
Only NL	69.8	60.8	52.1	80.4	60.9	50.3	70.4	57.8	54.0	61.8

Table 1. Object detection average precision (%) on KITTI dataset using different models. Ground Truth: results of model trained on ground truth labeled data (comes from KITTI). New labeled and ground truth: model trained on both new labeled data and ground truth data, corresponding to experiment 1. Sampled NL and GT: model trained on importance sampled new labeled data and ground truth data, corresponding to experiment 2. Only NL: model trained only on new labeled data, corresponding to experiment 3.

4. Experiments

Our framework has several major contributions. First of all, we proposed to use object tracker’s prediction as the region proposal input for the object detection network to detect objects. Secondly, we proposed to use near-to-far labeling to help correct labels that may not be correct. Thirdly, we use importance sampling to select an optimal subset of images to remove images with less reliable labels and obtain a smaller but more informative set of data. We designed several comparative experiments to show the impact of our contribution.

4.1. Comparative Experiments

Datasets. To show that our algorithm is able to scale to a relatively large video dataset, we choose the KITTI benchmark dataset [13] which contains hundreds of autonomous driving video clips, and each of the video clips lasts about 10 to 30 seconds. The data set is fairly rich as it contains high-resolution color and grayscale video frames captured in many kinds of driving environments: city, residential, road, campus, person, etc. The KITTI dataset also contains a set of sparsely labeled image frames for object detection purposes. The number of images with ground truth bounding box labeling we used in our experiment is 7481, while the total number of images is around 40000. Categories of objects being labeled include cars, pedestrians, vans, trams, cyclist, truck, person sitting, and so on. For simplicity, we choose 3 categories from them to detect, which include cars, pedestrians, and cyclist. We manually and randomly divide the dataset into the training, validation and test data set. The

training dataset contains 4206 images, the validation dataset contains 1404 images, and the test data set contains 1871 images.

Experiment 0. We first trained a basic object detection network based on the ground truth labeled data using the Faster-RCNN [26] object detection network. As for details of training, we used pre-trained Faster-RCNN model with VGG16 network [32] trained on PASCAL VOC 2007 dataset [11], and then finetuned with KITTI dataset. The number of training iterations is 300k with the initial learning rate of 0.01 and decay every 30k iterations.

Experiment 1. The first experiment is our labeling by tracking approach using semi-supervised learning. In this experiment, we use the ground truth labeled bounding boxes to initialize object trackers. Since images in the KITTI dataset are sparsely labeled with unlabeled images between labeled images in the original video sequence, we use the labeled data as a guidance to label images without ground truth labeling. It is useful to notice that, in this case, the object detection network does not use RPN to generate region proposals. Instead, it takes the object tracker’s prediction of bounding box in the next frame as region proposal and then perform bounding box regression to generate optimal bounding box for the object being tracked. In other words, only ground truth labeled images can be used to initialize object tracker, which is based on our assumption that objects in the near field provide more accurate information and we only predict bounding boxes based on reliable information instead of relying on some random detection. We used both ground truth data from KITTI combined with new la-

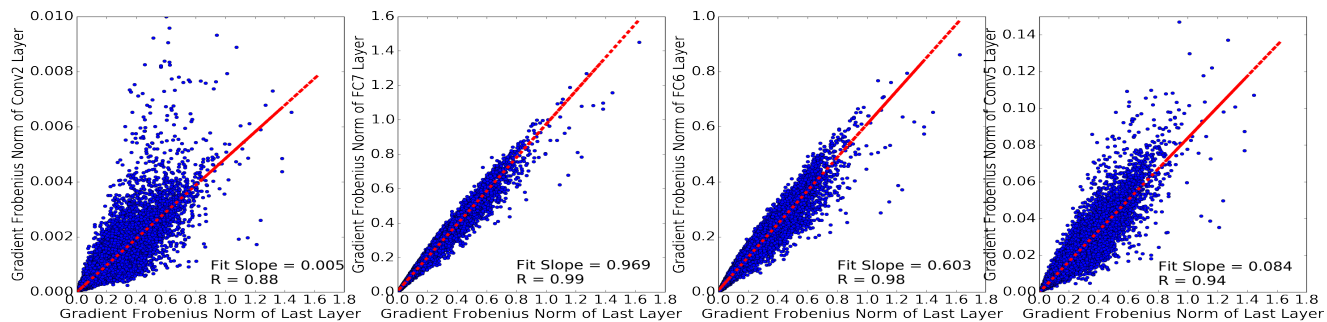


Figure 3. Plot of gradient Frobenius norm of last layer in VGG 16 versus the gradient Frobenius norm of fully-connected layer 7 (FC7), fully-connected layer 6(FC6), Convolutional Layer 5 (Conv5) and Convolutional Layer 1 (Conv1).



Figure 4. Examples of near-to-far labeling. These images are from the KITTI Benchmark data set [13]. The labeling results are obtained from pre-trained Faster-RCNN model. The bounding box shows the detected objects being tracked. Near field object detection results are used to check the accuracy of the detection results of objects in the far field. The first image labeling results from left to right: motorbike, car, car (ground truth). As the vehicle approaches the object, it becomes clearer and no longer hidden by the pole. The second image labeling results from left to right: bus, car, train (ground truth). The object looks like a bus in the far field, but is classified as train when it's in the near field considering it's on railroad. The third image labeling results from left to right: train, car, car (ground truth). The object looks like a train in the far field, but is classified as car when it's in the near field. Fourth image labeling results from left to right: bus, car, car (ground truth). At first sight, the car is blurred and hidden by other objects, then it became more clearer that this is a car.

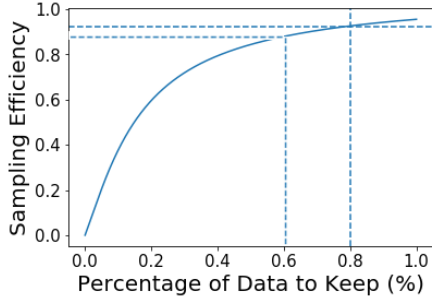


Figure 5. Relative Variance Evaluation Results

beled data to train the object detector. The training setting is the same as in experiment 0.

Experiment 2. In this experiment, we adopt the approach we take in experiment 1 and we further combine it with importance sampling. As images labeled using the approach in experiment 1 may still contain redundant information such as images that are already easy for the network to process, so we use importance sampling to select an optimal set of images that are more informative. We choose to sample 60% of the data (which consists of both ground truth and new labeled data) in experiment 1 using the importance sampling method mentioned in previous section. As shown in figure 5, 60% of data corresponds to around 0.90 sampling efficiency, which is reasonably high. The training setting is also the same as in experiment 0.

Experiment 3. We further remove the ground truth data which comes from KITTI and only used newly labeled data using to train an object detector with the same training setting as in experiment 0.

Evaluation of Accuracy. We trained Faster-RCNN object detection networks using data mentioned in experiment 1, 2, and 3 respectively, all using the same training configurations as we did in experiment 0. We evaluate the performance of models in experiment 0,1,2,and 3 by testing the models on a held out test dataset of 1871 images. The average precision is evaluated on the 3 categories of objects mentioned before.

4.2. Results and Analysis

Loss as a Approximation for Gradient First, we show our finding that the gradient of the network we used has some linear correlation between different layers as shown in figure 3. Therefore, we can use last layer gradient (as it is easier to obtain) as a approximation of total gradients. On the other hand, we also show in figure 6 that loss can be used as a approximation for the total gradient norm. Therefore, we can also use loss to approximate gradient and use it as sampling weight for different object bounding box labels.

Qualitative Results for Bounding Box Generation. As mentioned in experiment description, we use two different strategies to generate bounding boxes using Faster-RCNN.

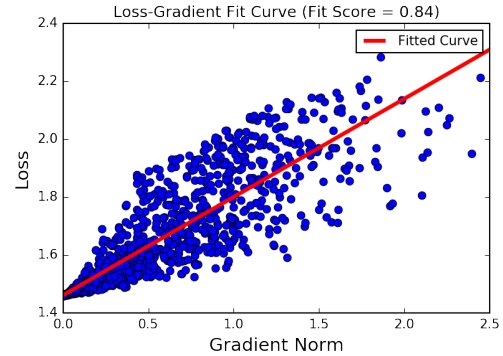


Figure 6. Plot of gradient Frobenius norm of entire network weight (not include bias term) VS the loss of individual data point.

The first strategy uses region proposal network to generate bounding boxes, and the second strategy uses object tracker’s prediction as region proposals. We show some qualitative results of bounding boxes generated by the two methods in figure 2.

Quantitative Results for Object Detection. The accuracy of models trained on experiment 0,1,2,and 3 are evaluated on a test data set of 1871 images. The average precision (AP) on 3 categories of objects and the mAPs are reported in table 1. The results show the average precision for different categories of objects with different degrees of difficulty. With the ground truth data, the model shows the best performance, which is not a surprise since labels generated by tracking may introduce noise that harms the performance of the detector. However, after filtering the data by importance sampling, we can obtain better detection accuracy using the same training setting, which means importance sampling has helped to reduce data volume and makes it easier to train a model to convergence.

Relative Variance Results We use the relative variance mentioned in section 3.3 to measure how good we estimate the image detection loss distribution. The result is shown here 5. From the plot, we can see that by scaling the importance sampling weight as mentioned in 5, we are able to keep high sampling efficiency (0.90) with 60 % of the original labeled data being sampled. This curve will be useful for determining how much data to sample given the desired sampling efficiency.

5. Conclusion

We proposed a framework of automatically generating object bounding box labels for large volume driving video dataset with sparse labels. Our work generates object bounding boxes on the new labeled data by employing a near-to-far labeling strategy, a combination of object tracker’s prediction and object detection network and the importance sampling scheme. Our experiments show that with our semi-supervised learning framework, we are able

to annotate driving video dataset with bounding box labels and improve the accuracy of object detection with the new labeled data using importance sampling.

References

- [1] Simple online and realtime tracking. In *2016 IEEE International Conference on Image Processing (ICIP)*, pages 3464–3468, Sept 2016.
- [2] G. Alain, A. Lamb, C. Sankar, A. Courville, and Y. Bengio. Variance reduction in sgd by distributed importance sampling. *arXiv preprint arXiv:1511.06481*, 2015.
- [3] J. Berclaz, F. Fleuret, E. Turetken, and P. Fua. Multiple object tracking using k-shortest paths optimization. *IEEE transactions on pattern analysis and machine intelligence*, 33(9):1806–1819, 2011.
- [4] A. Bewley, Z. Ge, L. Ott, F. Ramos, and B. Upcroft. Simple online and realtime tracking. *CoRR*, abs/1602.00763, 2016.
- [5] M. D. Breitenstein, F. Reichlin, B. Leibe, E. Koller-Meier, and L. Van Gool. Robust tracking-by-detection using a detector confidence particle filter. In *Computer Vision, 2009 IEEE 12th International Conference on*, pages 1515–1522. IEEE, 2009.
- [6] J. Choi, M. Rastegari, A. Farhadi, and L. S. Davis. Adding unlabeled samples to categories by learned attributes. In *Proceedings of the IEEE Conference on Computer Vision and Pattern Recognition*, pages 875–882, 2013.
- [7] D. Csiba and P. Richtárik. Importance sampling for mini-batches. *arXiv preprint arXiv:1602.02283*, 2016.
- [8] J. Deng, W. Dong, R. Socher, L.-J. Li, K. Li, and L. Fei-Fei. Imagenet: A large-scale hierarchical image database. In *Computer Vision and Pattern Recognition, 2009. CVPR 2009. IEEE Conference on*, pages 248–255. IEEE, 2009.
- [9] J. Duchi and Y. Singer. Efficient online and batch learning using forward backward splitting. *Journal of Machine Learning Research*, 10(Dec):2899–2934, 2009.
- [10] J. C. Duchi, S. Shalev-Shwartz, Y. Singer, and A. Tewari. Composite objective mirror descent. In *COLT*, pages 14–26, 2010.
- [11] M. Everingham, L. Van Gool, C. K. Williams, J. Winn, and A. Zisserman. The pascal visual object classes (voc) challenge. *International journal of computer vision*, 88(2):303–338, 2010.
- [12] R. Farah, Q. Gan, J. P. Langlois, G.-A. Bilodeau, and Y. Savaria. A computationally efficient importance sampling tracking algorithm. *Machine Vision and Applications*, 25(7):1761–1777, 2014.
- [13] A. Geiger, P. Lenz, and R. Urtasun. Are we ready for autonomous driving? the kitti vision benchmark suite. In *Computer Vision and Pattern Recognition (CVPR), 2012 IEEE Conference on*, pages 3354–3361. IEEE, 2012.
- [14] R. Girshick, J. Donahue, T. Darrell, and J. Malik. Rich feature hierarchies for accurate object detection and semantic segmentation. In *Computer Vision and Pattern Recognition*, 2014.
- [15] R. B. Girshick. Fast R-CNN. *CoRR*, abs/1504.08083, 2015.
- [16] H. Grabner, C. Leistner, and H. Bischof. Semi-supervised on-line boosting for robust tracking. In *European conference on computer vision*, pages 234–247. Springer, 2008.
- [17] Z. Kalal, K. Mikolajczyk, and J. Matas. Tracking-learning-detection. *IEEE transactions on pattern analysis and machine intelligence*, 34(7):1409–1422, 2012.
- [18] S. Lad and D. Parikh. Interactively guiding semi-supervised clustering via attribute-based explanations. In *European Conference on Computer Vision*, pages 333–349. Springer, 2014.
- [19] D. Liu, G. Hua, and T. Chen. A hierarchical visual model for video object summarization. *IEEE transactions on pattern analysis and machine intelligence*, 32(12):2178–2190, 2010.
- [20] W. Liu, D. Anguelov, D. Erhan, C. Szegedy, S. E. Reed, C. Fu, and A. C. Berg. SSD: single shot multibox detector. *CoRR*, abs/1512.02325, 2015.
- [21] I. Misra, A. Shrivastava, and M. Hebert. Watch and learn: Semi-supervised learning of object detectors from videos. *CoRR*, abs/1505.05769, 2015.
- [22] Y. Z. Owen, Art; Associate. Safe and effective importance sampling. *Journal of the American Statistical Association*, 449:135 – 143, 2000.
- [23] H. Pirsiavash, D. Ramanan, and C. C. Fowlkes. Globally-optimal greedy algorithms for tracking a variable number of objects. In *Computer Vision and Pattern Recognition (CVPR), 2011 IEEE Conference on*, pages 1201–1208. IEEE, 2011.
- [24] A. Prest, C. Leistner, J. Civera, C. Schmid, and V. Ferrari. Learning object class detectors from weakly annotated video. In *Computer Vision and Pattern Recognition (CVPR), 2012 IEEE Conference on*, pages 3282–3289. IEEE, 2012.
- [25] J. Redmon, S. K. Divvala, R. B. Girshick, and A. Farhadi. You only look once: Unified, real-time object detection. *CoRR*, abs/1506.02640, 2015.
- [26] S. Ren, K. He, R. B. Girshick, and J. Sun. Faster R-CNN: towards real-time object detection with region proposal networks. *CoRR*, abs/1506.01497, 2015.
- [27] E. Romera, L. M. Bergasa, and R. Arroyo. Can we unify monocular detectors for autonomous driving by using the pixel-wise semantic segmentation of cnns? *CoRR*, abs/1607.00971, 2016.
- [28] R. Y. Rubinstein and D. P. Kroese. *Simulation and the Monte Carlo method*, volume 707. John Wiley & Sons, 2011.
- [29] S. Shalev-Shwartz and T. Zhang. Proximal stochastic dual coordinate ascent. *arXiv preprint arXiv:1211.2717*, 2012.
- [30] A. Shrivastava, A. Gupta, and R. Girshick. Training region-based object detectors with online hard example mining. In *Proceedings of the IEEE Conference on Computer Vision and Pattern Recognition*, pages 761–769, 2016.
- [31] A. Shrivastava, S. Singh, and A. Gupta. Constrained semi-supervised learning using attributes and comparative attributes. In *European Conference on Computer Vision*, pages 369–383. Springer, 2012.
- [32] K. Simonyan and A. Zisserman. Very deep convolutional networks for large-scale image recognition. *CoRR*, abs/1409.1556, 2014.

- [33] K. Tang, R. Sukthankar, J. Yagnik, and L. Fei-Fei. Discriminative segment annotation in weakly labeled video. In *Proceedings of the IEEE conference on computer vision and pattern recognition*, pages 2483–2490, 2013.
- [34] Y. Tang, J. Wang, B. Gao, E. Dellandréa, R. Gaizauskas, and L. Chen. Large scale semi-supervised object detection using visual and semantic knowledge transfer. In *Proceedings of the IEEE Conference on Computer Vision and Pattern Recognition*, pages 2119–2128, 2016.
- [35] A. Teichman and S. Thrun. Practical object recognition in autonomous driving and beyond. *Advanced Robotics and its Social Impacts (ARSO), 2011 IEEE Workshop on*, pages 35–38, 10 2011.
- [36] N. Wang and D. yan Yeung. Learning a deep compact image representation for visual tracking. In C. Burges, L. Bottou, M. Welling, Z. Ghahramani, and K. Weinberger, editors, *Advances in Neural Information Processing Systems 26*, pages 809–817. 2013.
- [37] G. Welch and G. Bishop. An introduction to the kalman filter. 1995.
- [38] T. Zhang and R. EDU. Stochastic optimization with importance sampling for regularized loss minimization. 2014.

Appendices

A. Introduction

We provide proof of the importance sampling framework and their optimality in this supplementary material. We also provide detailed explanations for the measurement of relative variance and the meaning of relative variance.

B. Importance Sampling Framework Proof

The importance sampling algorithm is used for data reduction. It is also used for the selection of an optimal subset of data from the original labeled dataset with minimal variance. In the paper, we stated that by using a reference proposal distribution $q^*(x) \propto p(x)|f(x)|$ we can get an estimation of the expectation of $f(x)$ with the least variance. We now provide the proof.

In importance sampling, the expectation of $f(x)$ is estimated by using $\mathbb{E}_{p(x)}[f(x)] = \mathbb{E}_{q(x)}[f(x)p(x)/q(x)]$. We require that $q(x) > 0$ whenever $f(x)p(x) \neq 0$. It is thus easily to verify that this estimation is unbiased. Suppose that $\mathbb{E}_{p(x)}[f(x)]$ is defined on $x \in A$ while $\mathbb{E}_{q(x)}[f(x)p(x)/q(x)]$ is defined on $x \in B$. We have $A = \{x|p(x) > 0\}$ and $B = \{x|q(x) > 0\}$. So that we have for $x \in A \cap B^c$, $f(x) = 0$ and for $x \in A^c \cap B$, $p(x) = 0$. That is to say, for $x \in A \cap B^c$ and $x \in A^c \cap B$, we have $f(x)p(x) = 0$. So the expectation of $f(x)$ can be written as,

$$\begin{aligned} \mathbb{E}_{q(x)}\left[\frac{p(x)f(x)}{q(x)}\right] &= \int_B \frac{f(x)p(x)}{q(x)}q(x)dx \\ &= \int_A f(x)p(x)dx + \int_{B \cap A^c} f(x)p(x)dx \\ &\quad - \int_{A \cap B^c} f(x)p(x)dx \\ &= \int_A f(x)p(x)dx \\ &= \mathbb{E}_{p(x)}[f(x)] \end{aligned} \quad (7)$$

Then we prove that when sampling distribution $q(x) \propto p(x)|f(x)|$, we can obtain the minimal variance in the estimation of the expectation. Let $\mathbb{E}_{p(x)}[f(x)] = \mu$, and let,

$$\mu_q = \frac{1}{n} \sum_{i=1}^n \frac{f(x_i)p(x_i)}{q(x_i)} \quad (8)$$

given samples x_i are sampled from $q(x)$. Then the variance of μ_q is,

$$\begin{aligned} \text{Var}(\mu_q) &= \frac{1}{n} \text{Var}\left(\frac{f(x_0)p(x_0)}{q(x_0)}\right) \\ &= \frac{1}{n} \left(\int (f(x)p(x))^2/q(x)dx - \mu^2 \right) \end{aligned} \quad (9)$$

By choosing $q^*(x) = |f(x)p(x)|/\mathbb{E}_p(|f(x)|)$, and let $q(x)$ be any density function that is positive given $f(x)p(x) \neq 0$. We have,

$$\begin{aligned} \text{Var}(\mu_q^*) &= \frac{1}{n} \left(\int \frac{(f(x)p(x))^2}{q^*(x)}dx - \mu^2 \right) \\ &= \frac{1}{n} \left(\int \frac{(f(x)p(x))^2}{|f(x)p(x)|/\mathbb{E}_p(|f(x)|)}dx - \mu^2 \right) \\ &= \frac{1}{n} \left(\mathbb{E}_p(|f(x)|)^2 - \mu^2 \right) \\ &= \frac{1}{n} \left(\mathbb{E}_q(|f(x)p(x)/q(x)|^2) - \mu^2 \right) \\ &\leq \frac{1}{n} \left(\mathbb{E}_q(f(x)^2p(x)^2/q(x)^2) - \mu^2 \right) \\ &= \text{Var}(\mu_q) \end{aligned} \quad (10)$$

The last inequality is the Cauchy-Schwarz inequality. Therefore, we show that by choosing sampling distribution $q(x) \propto p(x)|f(x)|$ and sampling data according to the normalized $q_{normalized}(x_i) = q(x_i)/\sum q(x_i)$, we can obtain the minimal variance estimation. In the case where $p(x)$ is not known directly, but we have a dataset sampled from $p(x)$, we can use $q(x_i) = |f(x_i)|/\sum_i |f(x_i)|$ as the sampling weight.

C. Measuring the Efficiency of Sampling

We define the efficiency as the ratio between the original data variance and the sampled data variance. To make things simpler, suppose we want to estimate the expectation of $f(x)$, we first normalize $f(x)$ and obtain $g(x) = (f(x) - \mathbb{E}[f(x)])/ \sigma[f(x)]$, where $\mathbb{E}[f(x)]$ and $\sigma[f(x)]$ are the mean and standard deviation of $f(x)$. Now we use importance sampling to estimate the expectation of $g(x)$ under $p(x)$ by using proposal distribution $q(x)$. We sample M images out of a total N images, the probability of a particular image x_i being sampled is,

$$s(x_i) = \min \left[1, \frac{M|g(x_i)|}{\sum_{i=1}^N |g(x_i)|} \right] \quad (11)$$

As mentioned in the paper, we take the minimum compared with 1 to ensure that the probability is always no more than 1. Obviously, $\sum_{i=1}^N s(x_i) > 1$ since $s(x_i)$ describes the probability of a particular image x_i being selected. We further define $q(x_i) = s(x_i)/N$ which has an upper bound of $1/N$. Therefore, it is easy to see that $\sum_{i=1}^N q(x_i) \leq 1$. To get M images, we select images according to their sampling probabilities $s(x_i)$. The expectation of $g(x)$ based on the sampled images is,

$$\mathbb{E}_{q(x)}[g(x)p(x)/q(x)] = \frac{1}{N} \sum_{i=1}^N g(x_i)p(x_i)/q(x_i) \quad (12)$$

where $x_i \sim q(x)$. On the other hand, if we sample the entire dataset and get N images, then $s(x_i) = 1$ and $q(x_i) = 1/N$, the expectation will be,

$$\mathbb{E}_{q(x)}[g(x)p(x)/q(x)] = \frac{1}{N} \sum_{i=1}^N g(x_i)p(x_i) * N \quad (13)$$

which is just $\mathbb{E}_{p(x)}[g(x)]$. It is no harm to assume $p(x)$ is a uniform distribution since we consider it to be unknown. In the case where we sample the entire dataset, $s(x_i) = 1$, $p(x_i) = 1/N$, and $\sum_{i=1}^N g(x_i) = 0$, then the variance of $g(x)$ by sampling the entire dataset is,

$$\begin{aligned} \text{Var}_q \left[\frac{g(x)p(x)}{q(x)} \right] &= \mathbb{E}_q \left[\left(\frac{g(x)p(x)}{q(x)} \right)^2 \right] - \left(\mathbb{E}_q \left[\frac{g(x)p(x)}{q(x)} \right] \right)^2 \\ &= \sum_{i=1}^N \left[\frac{g(x_i)p(x_i)}{s(x_i)/N} \right]^2 \frac{s(x_i)}{N} \\ &\quad - \left(\sum_{i=1}^N \left[\frac{g(x_i)p(x_i)}{s(x_i)/N} \right] \frac{s(x_i)}{N} \right)^2 \\ &= \sum_{i=1}^N \left[\frac{g(x_i)/N}{1/N} \right]^2 \frac{1}{N} \\ &\quad - \left(\sum_{i=1}^N g(x_i)/N \right)^2 \\ &= \sum_{i=1}^N g^2(x_i)/N \end{aligned} \quad (14)$$

In the case where we sample M images out of N images, $s(x_i) \leq 1$, $q(x_i) = 1/N$, and $\sum_{i=1}^N g(x_i) = 0$, then the variance of $g(x)$ by sampling M images out of N images is,

$$\begin{aligned} \text{Var}_{q(x)} \left[\frac{g(x)p(x)}{q(x)} \right] &= \sum_{i=1}^N \left[\frac{g(x_i)p(x_i)}{s(x_i)/N} \right]^2 \frac{s(x_i)}{N} \\ &\quad - \left(\sum_{i=1}^N \left[\frac{g(x_i)p(x_i)}{s(x_i)/N} \right] \frac{s(x_i)}{N} \right)^2 \\ &= \sum_{i=1}^N \left[\frac{g(x_i)/N}{s(x_i)/N} \right]^2 \frac{s(x_i)}{N} \\ &\quad - \left(\sum_{i=1}^N g(x_i)/N \right)^2 \\ &= \sum_{i=1}^N \frac{g^2(x_i)}{s(x_i) * N} \end{aligned} \quad (15)$$

The efficiency is defined as the ratio between 14 and 15, which is,

$$R = \frac{\sum_{i=1}^N g^2(x_i)}{\sum_{i=1}^N g^2(x_i)/s(x_i)} \quad (16)$$

which is the same as the efficiency (relative variance) defined in the main paper. Obviously, since $s(x_i) \leq 1$, this ratio will always be no larger than 1. If we sample all the data, which means $s(x_i) = 1$, then we can obtain a sampling efficiency of 1. To simplify the calculation of R , We can further express $\sum_{i=1}^N g^2(x_i)/s(x_i)$ as,

$$\begin{aligned} \sum_{i=1}^N \frac{g^2(x_i)}{s(x_i)} &= \sum_{j=1}^k \frac{\sum_{i=1}^N |g(x_i)|}{M|g(x_j)|} |g(x_j)|^2 + \sum_{j=k+1}^N |g(x_j)|^2 \\ &= \frac{\sum_{i=1}^N |g(x_i)|}{M} \left(\sum_{j=1}^k |g(x_j)| \right) + \sum_{j=k+1}^N |g(x_j)|^2 \end{aligned} \quad (17)$$

where $s(x_1), s(x_2), \dots, s(x_k)$ are smaller than 1 and $s(x_{k+1}), \dots, s(x_N)$ are equal to 1.